Letter

Complex Hydrogen Substructure in Semimetallic RuH$_4$

Jack Binns, Yu He, Mary-Ellen Donnelly, Miriam Peña-Alvarez, Mengnan Wang, Duck Young Kim, Eugene Gregoryanz, Philip Dalladay-Simpson, and Ross T. Howie*
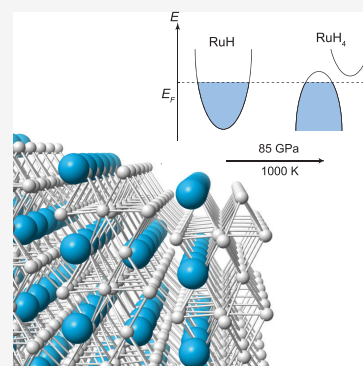
HPSTAR
997-2020

Read Online

ACCESS | Metrics & More | Article Recommendations | Supporting Information

ABSTRACT: When compressed in a matrix of solid hydrogen, many metals form compounds with increasingly high hydrogen contents. At high density, hydrogenic sublattices can emerge, which may act as low-dimensional analogues of atomic hydrogen. We show that at high pressures and temperatures, ruthenium forms polyhydride species that exhibit intriguing hydrogen substructures with counterintuitive electronic properties. Ru$_3$H$_8$ is synthesized from RuH in H$_2$ at 50 GPa and at temperatures in excess of 1000 K, adopting a cubic structure with short H−H distances. When synthesis pressures are increased above 85 GPa, we observe RuH$_4$ which crystallizes in a remarkable structure containing corner-sharing H$_6$ octahedra. Calculations indicate this phase is semimetallic at 100 GPa.

The physical properties of a host metal can be profoundly altered by the presence of hydrogen. Examples include switchable mirrors driven by an electronic transition,[1,2] the disruption of magnetic ordering,[3−6] and the dramatic increases in superconducting transition temperatures (T_c) for metallic hydrides at high pressures ($P > 200$ GPa).[7−10] The solubility of hydrogen in transition metals increases rapidly under compression, with polyhydride species being discovered in a number of first- and second-row members of the group[11−18] and predicted for many others.[19−22] As hydrogen content increases, intriguing substructures emerge, taking the form of H$_3^-$ quasimolecules, clathrate cages, and layers of isolated H atoms.[13,19,23−28] Unique to group 8 metals (Fe, Ru, Os), it has been predicted that increasing hydrogen content should lead to the emergence of a series of nonmetallic hydrides FeH$_4$,[29] FeH$_6$,[30] FeH$_7$,[28] RuH$_6$,[31] and OsH$_6$.[24] Despite intensive study of the Fe−H system, none of these materials has been synthesized due to the very high pressures (i.e., >200 GPa) required to stabilize them. Ruthenium polyhydride structures are predicted to emerge at much lower pressures, making it ideal to study the formation and properties of nonmetallic hydrides.

Ruthenium monohydride (RuH) has been shown to form at pressures above 14 GPa at room temperature by reaction of its constituent elements and remains stable to at least 30 GPa.[32] Theoretical structure searches predict the emergence of stable compounds with stoichiometries of RuH$_3$ and RuH$_6$, the latter containing molecular H$_2$ and becoming unstable above 100 GPa.[31]

Here, we report the formation of two new ruthenium polyhydride species synthesized using a combination of high temperatures and pressures. On compression, we observe the formation of the known hydride RuH and confirm its stability up to 100 GPa. After heating RuH in a matrix of solid H$_2$ at pressures above 50 GPa, new diffraction peaks appear, which we determine to be due to Ru$_3$H$_8$, which decomposes below 20 GPa. After heating in H$_2$ at pressures above 85 GPa, RuH partially transforms to a second novel phase, RuH$_4$, which remains stable down to 70 GPa. Through a combination of X-ray diffraction and DFT calculations, we characterized the structures and electronic properties of this material. RuH$_4$ is found to contain atomic hydrogen arranged in corner-sharing octahedra. Our calculations indicate that this material is a semimetal at 100 GPa.
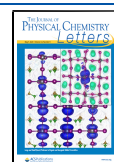
After gas loading at 0.2 GPa, mixtures of Ru and H$_2$ were compressed to 15 GPa, and in agreement with a previous study, we observe the formation of RuH by compression alone (Figure 1(a)).[32] RuH crystallizes in a face-centered cubic structure (space group $Fm\bar{3}m$, $a = 3.8650(1)$ Å at 33 GPa) isostructural to other transition metal monohydrides (e.g., CoH, RhH, NiH).[14,15,17] In the absence of heating, we find RuH remains stable to pressures of 100 GPa.
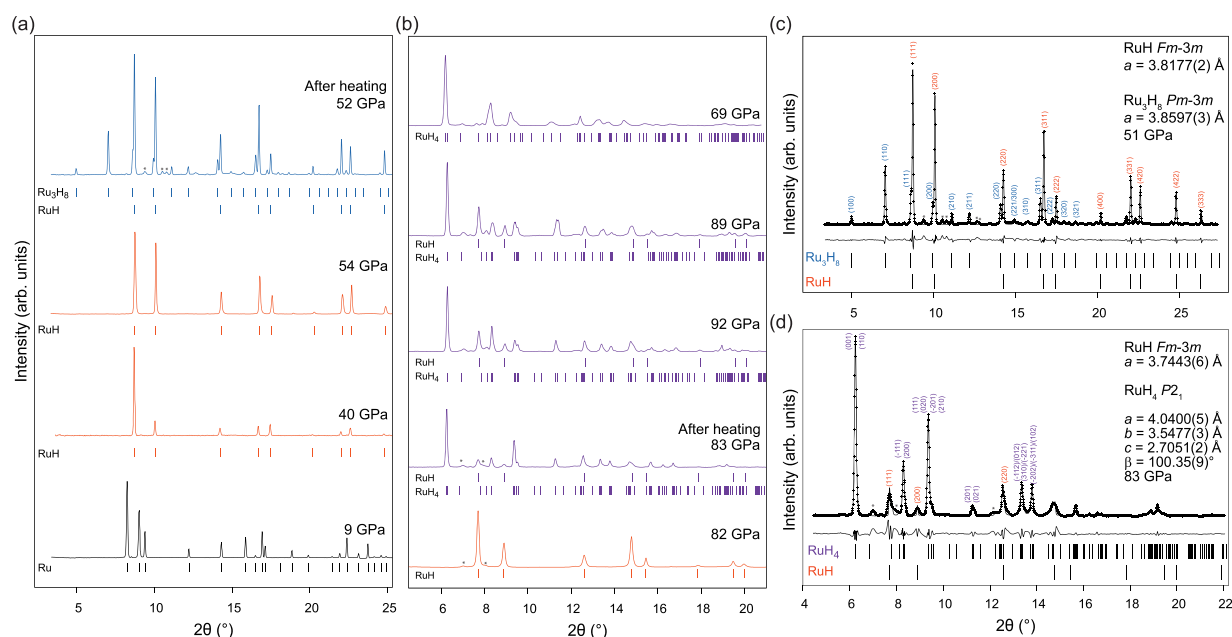
In situ laser heating has been shown to be a highly effective route to reaching new transition metal hydrides[11,13−16] and was applied here to explore the formation of predicted ruthenium polyhydrides. Samples of RuH and H$_2$ were
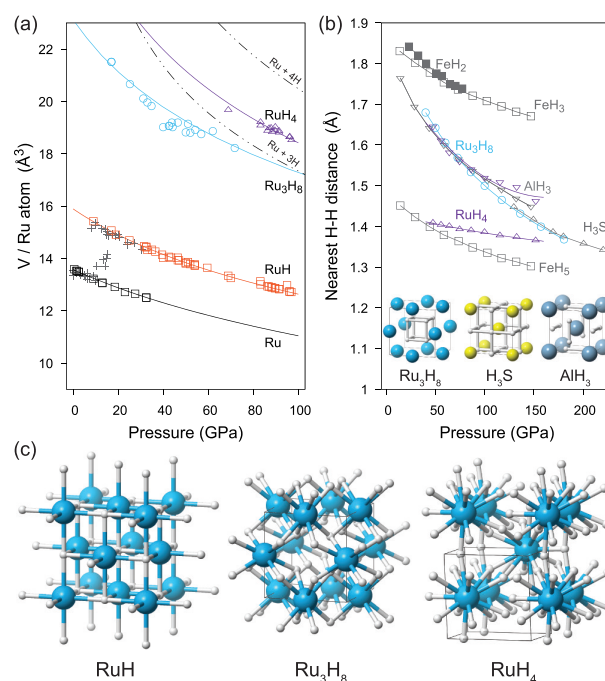
Figure 1. Representative X-ray diffraction patterns of Ru polyhydrides (a) after laser heating at 51 GPa, additional peaks due to Ru_3H_8 can be observed (λ = 0.3344 Å). (b) At higher pressures of 89 GPa, heating RuH + H_2 results in additional peaks indexed to a monoclinic unit cell due to RuH_4 (λ = 0.2897 Å). (c, d) Representative Le Bail refinements of RuH + Ru_3H_8 (λ = 0.3344 Å) and RuH + RuH_4 (λ = 0.2897 Å). Tick marks indicate Bragg peaks for the noted phases. Peaks due to ReH gasket are marked with (*).

compressed and at pressures above 50 GPa laser heated to temperatures over 1500 K, leading to the appearance of new diffraction peaks in addition to those of RuH (Figure 1(a)). All of the new diffraction peaks could be indexed to a primitive cubic unit cell a = 3.8352(3) Å. Structure solution by charge-flipping[33] suggested the presence of a single Ru atom site $3g$ $\left(\frac{1}{2}, 0, 0\right)$. Analysis of the volume per Ru atom (Figure 2(a)) suggested a stoichiometry of RuH_3. Samples were subsequently compressed and decompressed to determine the stability range, finding this new phase to be stable up to pressures of at least 71 GPa and down to 17 GPa before decomposing back into RuH + H_2.

Although a RuH_3 phase exhibiting a primitive cubic structure ($Pm\bar{3}m$, a = 2.598 Å at 100 GPa) has been predicted,[31] our experimental diffraction patterns clearly display additional reflections at low angles, which can only be explained with a larger unit cell. To understand this discrepancy, we performed our own structure searching calculations using noninteger values of H/Ru and directed by the experimental lattice constants. These calculations found a stable compound with stoichiometry Ru_3H_8, which shows excellent agreement between calculated and observed unit cell dimensions and volume per Ru atom (Figure 2(a) and S1).

Calculations indicate that our observed Ru_3H_8 structure lies on the convex hull and is 0.446 eV per Ru atom more favorable than RuH_3, as predicted by ref 31, which lies 0.01 eV above at 70 GPa (Figure S2). In Ru_3H_8, each Ru atom is coordinated by eight H atoms with equal Ru–H bonds (1.805 Å at 70 GPa). Remarkably, each unit cell contains a cubic H_8 unit at the center with H–H distances (at 70 GPa) of 1.616 Å along each cube edge. These isolated units result in H–H distances that are significantly shorter than comparable phases such as FeH_3[12] and in fact track closely to those of the molecular hydrides AlH_3 and H_3S.[34,35] Unlike these compounds, the close H–H distances are not part of a continuous network but
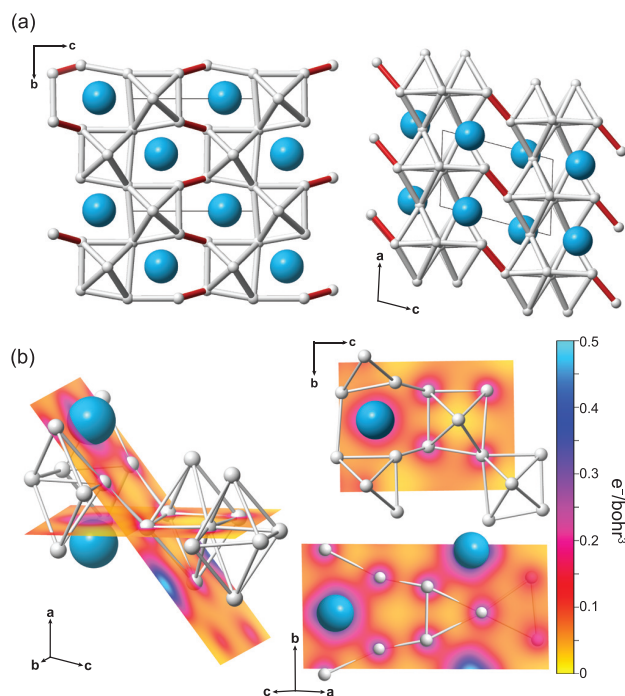

Figure 2. (a) Volume per Ru atom for various Ru−H compounds. Crosses refer to previous study.[32] (b) Nearest H−H interatomic distances in various hydrogen-bearing materials at high pressures.[13,34,35] Inset shows corresponding hydrogen substructures. (c) Crystal structures of Ru−H compounds RuH, Ru_3H_8, and RuH_4. Ru atoms are blue; H atoms are white.

instead remain discrete units within the crystal structure (Figure 2(b)). Considering the H_8 cluster as a single unit at the unit cell center, the structure of Ru_3H_8 is analogous to the Cu_3Au-type structure. This structure type is a superstructure of the familiar fcc packing, which suggests that Ru atoms and H_8

clusters have comparable sizes under these conditions.[36] Calculations show Ru_3H_8 to be metallic and dynamically stable in the observed pressure regime (Figure S3 and S4).

Applying the same heating regime to mixtures of RuH + H_2 at pressures above 82 GPa caused new diffraction peaks to appear, indicating the formation of a second novel high pressure ruthenium polyhydride. All diffraction peaks could be fitted with a C-centered monoclinic cell (a = 4.0400(5), b = 3.5477(3), c = 2.7051(2) Å, β = 100.35(9)° at 83 GPa). This unit cell was used to constrain structure-searching calculations which explored stoichiometries with H/Ru > 3 (Figure 2(a)), finding a dynamically stable solution with stoichiometry RuH_4 and space group symmetry $P2_1$ (Figures 2(c) and 3(a)).
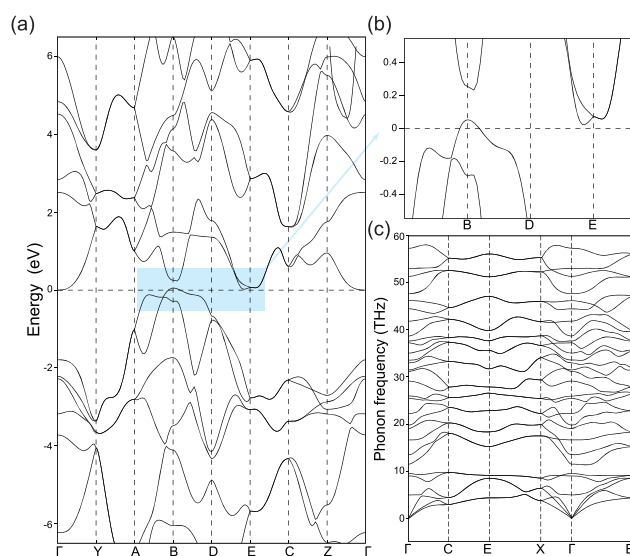

Figure 3. (a) Hydrogen sublattice in RuH_4, white "bonds" are shown between H atoms as a guide to the eye to highlight the structure of octahedral clusters. Short H−H distances between clusters are shown in red. (b) Two representative planes of the electron density distribution in RuH_4 are shown in relation to the crystal structure; (right) electron density maps through key aspects of the H_6 units.

Samples were compressed up to 100 GPa and subsequently decompressed to evaluate the equation of state and stability of this new compound, finding it to be stable down to at least 69 GPa, and changes in unit cell dimensions are in close agreement with calculations (Figure S5 and Table S1). At 70 GPa, RuH_4 is metastable, lying 0.027 eV/f.u. above the convex hull; this deviation is decreased at higher pressures reducing to 0.014 eV/f.u. at 100 GPa (Figure S2). It should be noted that other predicted metastable hydride phases have been synthesized to date, e.g.[37] RuH_4 adopts an entirely new structure type, analogous to the postulated γ-phase of FeH_4, predicted to occur at pressures above 240 GPa but which has remained elusive in experimental studies to date.[29,36]

In RuH_4, each Ru atom is coordinated by 12 H atoms forming highly irregular polyhedra with Ru−H interatomic distances ranging from 1.644 to 1.965 Å (at 100 GPa). However, the remarkable nature of this structure is made clear when we examine the H−H nearest neighbor distances,

highlighted with "bonds" to guide the eye in Figure 3(a). Ru atoms are arranged in channels along the a axis with H atoms forming layers of corner-sharing octahedra extending along the b axis. Each layer is two octahedra wide and staggered along a, linked by close H−H distances of 1.385 Å (shown in red Figure 3(a)). The calculated electron density distribution (Figure 3(b)) provides a qualitative indication of the bonding within RuH_4 and in particular the nature of the H_6 octahedra. As expected from other transition metal hydrides, bonding primarily occurs between Ru and H atoms. Examining slices through the H_6 clusters shows the absence of electron density between H atoms, clearly indicating that no H−H bonding is present, either within the H_6 octahedra or along the short H−H links between clusters, confirming the atomic nature of hydrogen in this structure.

Electronic structure calculations were conducted using the HSE hybrid functional which corrects for the known systematic underestimation of band gap energies by standard GGA functionals.[38,39] Calculated electronic band structures indicate that RuH_4 is semimetallic at 100 GPa (Figure 4). To

Figure 4. (a) Electronic band structure of RuH_4 at 100 GPa calculated with the HSE06 functional. (b) Region of the Fermi level highlighted. (c) Phonon dispersion curves for RuH_4 at 100 GPa.

our knowledge, RuH_4 is the first experimentally observed semimetallic transition-metal hydride. It is intriguing to note that although a nonmetallic ruthenium hydride has been predicted, it shares no structural relation to RuH_4 and instead contains molecular H_2 units.[31]

Current understanding of the mechanism of high T_c hydrides relies on the coupling of metallic conduction and high hydrogen content.[7] The emergence of complex hydrogen substructures is correlated to a reduction in metallic conduction, strongly suggesting that late transition metals likely provide a poor route to high T_c materials in line with recent critical analyses.[40]

We have demonstrated the formation of a remarkably complex hydrogen sublattice in RuH_4, synthesized at pressures of 85 GPa and temperatures of 1500 K. This structure contains layers of corner-sharing H_6 octahedra surrounding isolated Ru atoms. Electronic structure calculations indicate this phase is semimetallic at 100 GPa. Our findings show that with

increasing hydrogen content and pressure, complex emergent atomic hydrogen structures become favorable with counter-intuitive effects on the electronic properties of transition-metal hydrides.

Experimental and Theoretical Methods. High purity ruthenium powder (99.9%, 1−2 μm particle size) from Alfa Aesar was placed into diamond-anvil cells (DACs) together with gold as a pressure marker and subsequently gas loaded with research-grade hydrogen gas (99.9999%) at 0.2 GPa.[41] Loading of hydrogen was confirmed by the observation of the hydrogen vibrational mode using a custom-built microfocused Raman system.[42] Rhenium gaskets were used to form the sample chamber in all experimental runs, diamond anvil culets ranged from 50 to 200 μm.

Ru samples were heated *in situ* from both sides uniaxially by directly coupling to an yttrium−aluminum−garnet (YAG) laser with wavelength λ = 1064 nm. Angle-dispersive X-ray diffraction patterns were recorded on PerkinElmer XRD21 and Mar345 image-plate detectors at the P02.2 ECB (PETRA, Germany) and ID15B (ESRF, France) beamlines with energies in the range 30−42 keV.[43] Two-dimensional image-plate data were integrated with DIOPTAS[44] to yield intensity vs 2θ plots. Patterns were indexed with CONOGRAPH,[45] and Le Bail[46] refinements were carried out in Jana2006.[47] Volume and linear equation of state parameters were determined using EoSFit 7.[48]

The electronic structure calculations were carried out at high pressures within the framework of density function theory (DFT) in conjunction with the projector augment wave method (PAW) as implemented in the VASP code.[49−52] We used Heyd−Scuseria−Ernzerhof (HSE06)[38] functional to determine the electronic properties of Ru−H compounds as the HSE06 functional was shown to predict much better electronic properties than the generalized gradient approximations (GGA). The cutoff energy of the plane wave was set to 800 eV, and Brillouin zone sampling was done on Monkhorst−Pack k-mesh with separations of 0.03 Å^{-1}. The 3p, 4s, and 3d and H 2s and 2p electrons are included in the valence space.

ASSOCIATED CONTENT

Ⓢ Supporting Information

The Supporting Information is available free of charge at https://pubs.acs.org/doi/10.1021/acs.jpclett.0c00688.

Equation of state parameters, electronic and phonon band structures, experimental and calculated unit cell parameters (PDF)

AUTHOR INFORMATION

Corresponding Author

Ross T. Howie − *Center for High Pressure Science and Technology Advanced Research (HPSTAR), Shanghai 201203, China*; Email: ross.howie@hpstar.ac.cn

Authors

Jack Binns − *Center for High Pressure Science and Technology Advanced Research (HPSTAR), Shanghai 201203, China;* ⓞ orcid.org/0000-0001-5421-6841

Yu He − *Center for High Pressure Science and Technology Advanced Research (HPSTAR), Shanghai 201203, China; Key Laboratory of High-Temperature and High-Pressure Study of the Earth's Interior, Institute of Geochemistry, Chinese Academy of Sciences, Guiyang, Guizhou 550081, China*

Mary-Ellen Donnelly − *Center for High Pressure Science and Technology Advanced Research (HPSTAR), Shanghai 201203, China*

Miriam Peña-Alvarez − *Centre for Science at Extreme Conditions and The School of Physics & Astronomy, The University of Edinburgh, Edinburgh EH9 3FD, United Kingdom;* ⓞ orcid.org/0000-0001-7056-7158

Mengnan Wang − *Center for High Pressure Science and Technology Advanced Research (HPSTAR), Shanghai 201203, China*

Duck Young Kim − *Center for High Pressure Science and Technology Advanced Research (HPSTAR), Shanghai 201203, China; Department of Chemistry, Pohang University of Science and Technology (POSTECH), Pohang 37673, Republic of Korea*

Eugene Gregoryanz − *Center for High Pressure Science and Technology Advanced Research (HPSTAR), Shanghai 201203, China; Centre for Science at Extreme Conditions and The School of Physics & Astronomy, The University of Edinburgh, Edinburgh EH9 3FD, United Kingdom*

Philip Dalladay-Simpson − *Center for High Pressure Science and Technology Advanced Research (HPSTAR), Shanghai 201203, China*

Complete contact information is available at:
https://pubs.acs.org/10.1021/acs.jpclett.0c00688

Notes
The authors declare no competing financial interest.

ACKNOWLEDGMENTS

REFERENCES

(1) Huiberts, J. N.; Griessen, R.; Rector, J. H.; Wijngaarden, R. J.; Dekker, J. P.; De Groot, D. G.; Koeman, N. J. Yttrium and lanthanum hydride films with switchable optical properties. *Nature* 1996, 380, 231−234.

(2) Den Broeder, F. J.; Van Der Molen, S. J.; Kremers, M.; Huiberts, J. N.; Nagengast, D. G.; Van Gogh, A. T.; Huisman, W. H.; Koeman, N. J.; Dam, B.; Rector, J. H.; et al. Visualization of hydrogen migration in solids using switchable mirrors. *Nature* 1998, 394, 656−658.

(3) Chaboy, J.; Piquer, C. Modification of the magnetic properties of the $R_2Fe_{14}B$ series (R = rare earth) driven by hydrogen absorption. *Physical Review B - Condensed Matter and Materials Physics* 2002, 66, 1−9.

(4) Fujita, A.; Fujieda, S.; Hasegawa, Y.; Fukamichi, K. Itinerant-electron metamagnetic transition and large magnetocaloric effects in $La(Fe_xSi_{1-x})_{13}$ compounds and their hydrides. *Physical Review B - Condensed Matter and Materials Physics* 2003, 67, 12.

(5) San, X.; Ma, Y.; Cui, T.; He, W.; Han, B.; Liu, B.; Zou, G. Pressure-induced magnetic transition in metallic nickel hydrides by ab initio pseudopotential plane-wave calculations. *Phys. Rev. B: Condens. Matter Mater. Phys.* **2006**, *74*, 1−4.

(6) Ying, J.; Zhao, J.; Bi, W.; Alp, E. E.; Xiao, Y.; Chow, P.; Shen, G.; Struzhkin, V. V. Magnetic phase diagram of ϵ'-FeH. *Phys. Rev. B: Condens. Matter Mater. Phys.* **2020**, *101*, 020405.

(7) Peng, F.; Sun, Y.; Pickard, C. J.; Needs, R. J.; Wu, Q.; Ma, Y. Hydrogen Clathrate Structures in Rare Earth Hydrides at High Pressures: Possible Route to Room-Temperature Superconductivity. *Phys. Rev. Lett.* **2017**, *119*, 1−6.

(8) Somayazulu, M.; Ahart, M.; Mishra, A. K.; Geballe, Z. M.; Baldini, M.; Meng, Y.; Struzhkin, V. V.; Hemley, R. J. Evidence for Superconductivity above 260 K in Lanthanum Superhydride at Megabar Pressures. *Phys. Rev. Lett.* **2019**, *122*, 027001.

(9) Drozdov, A.; Kong, P.; Minkov, V.; Besedin, S.; Kuzovnikov, M.; Mozaffari, S.; Balicas, L.; Balakirev, F.; Graf, D.; Prakapenka, V. Superconductivity at 250 K in lanthanum hydride under high pressures. *Nature* **2019**, *569*, 528−531.

(10) Zurek, E.; Bi, T. High-temperature superconductivity in alkaline and rare earth polyhydrides at high pressure: A theoretical perspective. *J. Chem. Phys.* **2019**, *150*, 050901.

(11) Marizy, A.; Geneste, G.; Loubeyre, P.; Guigue, B.; Garbarino, G. Synthesis of bulk chromium hydrides under pressure of up to 120 GPa. *Phys. Rev. B: Condens. Matter Mater. Phys.* **2018**, *97*, 1−7.

(12) Pépin, C. M.; Dewaele, A.; Geneste, G.; Loubeyre, P.; Mezouar, M. New iron hydrides under high pressure. *Phys. Rev. Lett.* **2014**, *113*, 265504.

(13) Pépin, C. M.; Geneste, G.; Dewaele, A.; Mezouar, M.; Loubeyre, P. Synthesis of FeH$_5$: A layered structure with atomic hydrogen slabs. *Science* **2017**, *357*, 382−385.

(14) Wang, M.; Binns, J.; Donnelly, M.-E.; Peña-Alvarez, M.; Dalladay-Simpson, P.; Howie, R. T. High pressure synthesis and stability of cobalt hydrides. *J. Chem. Phys.* **2018**, *148*, 144310.

(15) Binns, J.; Donnelly, M.-E.; Wang, M.; Hermann, A.; Gregoryanz, E.; Dalladay-Simpson, P.; Howie, R. T. Synthesis of Ni$_2$H$_3$ at high temperatures and pressures. *Phys. Rev. B: Condens. Matter Mater. Phys.* **2018**, *98*, 1−4.

(16) Binns, J.; Peña-Alvarez, M.; Donnelly, M.-E.; Gregoryanz, E.; Howie, R. T.; Dalladay-Simpson, P. Structural Studies on the Cu−H System under Compression. *Engineering* **2019**, *5*, 505−509.

(17) Li, B.; Ding, Y.; Kim, D. Y.; Ahuja, R.; Zou, G.; Mao, H.-k. Rhodium dihydride (RhH$_2$) with high volumetric hydrogen density. *Proc. Natl. Acad. Sci. U. S. A.* **2011**, *108*, 18618−18621.

(18) Bi, T.; Zarifi, N.; Terpstra, T.; Zurek, E. The Search for Superconductivity in High Pressure Hydrides. In *Reference Module in Chemistry*; Molecular Sciences and Chemical Engineering: 2019.

(19) Kvashnin, A. G.; Kruglov, I. A.; Semenok, D. V.; Oganov, A. R. Iron Superhydrides FeH$_5$ and FeH$_6$: Stability, Electronic Properties, and Superconductivity. *J. Phys. Chem. C* **2018**, *122*, 4731−4736.

(20) Gao, G.; Wang, H.; Zhu, L.; Ma, Y. Pressure-Induced Formation of Noble Metal Hydrides. *J. Phys. Chem. C* **2012**, *116*, 1995−2000.

(21) Wang, L.; Duan, D.; Yu, H.; Xie, H.; Huang, X.; Tian, F.; Liu, B.; Cui, T. High-Pressure Formation of Cobalt Polyhydrides: A First-Principle Study. *Inorg. Chem.* **2018**, *57*, 181−186.

(22) Zaleski-Ejgierd, P.; Labet, V.; Strobel, T. A.; Hoffmann, R.; Ashcroft, N. W. WH$_n$ under pressure. *J. Phys.: Condens. Matter* **2012**, *24*, 155701.

(23) Wang, H.; Tse, J. S.; Tanaka, K.; Iitaka, T.; Ma, Y. Superconductive sodalite-like clathrate calcium hydride at high pressures. *Proc. Natl. Acad. Sci. U. S. A.* **2012**, *109*, 6463−6466.

(24) Liu, Y.; Duan, D.; Huang, X.; Tian, F.; Li, D.; Sha, X.; Wang, C.; Zhang, H.; Yang, T.; Liu, B.; et al. Structures and Properties of Osmium Hydrides under Pressure from First Principle Calculation. *J. Phys. Chem. C* **2015**, *119*, 15905−15911.

(25) Wang, Z.; Wang, H.; Tse, J. S.; Iitaka, T.; Ma, Y. Stabilization H$_3^+$ of in the high pressure crystalline structure of H$_n$Cl (n = 2−7). *Chem. Sci.* **2015**, *6*, 522−526.

(26) Struzhkin, V. V.; Kim, D. Y.; Stavrou, E.; Muramatsu, T.; Mao, H.-k.; Pickard, C. J.; Needs, R. J.; Prakapenka, V. B.; Goncharov, A. F. Synthesis of sodium polyhydrides at high pressures. *Nat. Commun.* **2016**, *7*, 12267.

(27) Liu, H.; Naumov, I. I.; Hoffmann, R.; Ashcroft, N. W.; Hemley, R. J. Potential high T_c superconducting lanthanum and yttrium hydrides at high pressure. *Proc. Natl. Acad. Sci. U. S. A.* **2017**, *114*, 6990−6995.

(28) Zarifi, N.; Bi, T.; Liu, H.; Zurek, E. Crystal Structures and Properties of Iron Hydrides at High Pressure. *J. Phys. Chem. C* **2018**, *122*, 24262−24269.

(29) Li, F.; Wang, D.; Du, H.; Zhou, D.; Ma, Y.; Liu, Y. Structural evolution of FeH$_4$ under high pressure. *RSC Adv.* **2017**, *7*, 12570.

(30) Zhang, S.; Lin, J.; Wang, Y.; Yang, G.; Bergara, A.; Ma, Y. Nonmetallic FeH$_6$ under High Pressure. *J. Phys. Chem. C* **2018**, *122*, 12022−12028.

(31) Liu, Y.; Duan, D.; Tian, F.; Wang, C.; Ma, Y.; Li, D.; Huang, X.; Liu, B.; Cui, T. Stability and properties of the Ru-H system at high pressure. *Phys. Chem. Chem. Phys.* **2016**, *18*, 1516−1520.

(32) Kuzovnikov, M. A.; Tkacz, M. Synthesis of ruthenium hydride. *Phys. Rev. B: Condens. Matter Mater. Phys.* **2016**, *93*, 064103.

(33) Oszlányi, G.; Süto, A. Ab initio structure solution by charge flipping. *Acta Crystallogr., Sect. A: Found. Crystallogr.* **2004**, *60*, 134−141.

(34) Goncharenko, I.; Eremets, M. I.; Hanfland, M.; Tse, J. S.; Amboage, M.; Yao, Y.; Trojan, I. A. Pressure-Induced Hydrogen-Dominant Metallic State in Aluminum Hydride. *Phys. Rev. Lett.* **2008**, *100*, 045504.

(35) Duan, D.; Liu, Y.; Tian, F.; Li, D.; Huang, X.; Zhao, Z.; Yu, H.; Liu, B.; Tian, W.; Cui, T. Pressure-induced metallization of dense (H$_2$S)$_2$H$_2$ with high T_c superconductivity. *Sci. Rep.* **2015**, *4*, 6968.

(36) Bazhanova, Z. G.; Oganov, A. R.; Gianola, O. Fe-C and Fe-H systems at pressures of the Earth's inner core. *Phys.-Usp.* **2012**, *55*, 489−497.

(37) Mishra, A. K.; Muramatsu, T.; Liu, H.; Geballe, Z. M.; Somayazulu, M.; Ahart, M.; Baldini, M.; Meng, Y.; Zurek, E.; Hemley, R. J. New calcium hydrides with mixed atomic and molecular hydrogen. *J. Phys. Chem. C* **2018**, *122*, 19370−19378.

(38) Heyd, J.; Scuseria, G. E.; Ernzerhof, M. Hybrid functionals based on a screened Coulomb potential. *J. Chem. Phys.* **2003**, *118*, 8207−8215.

(39) Heyd, J.; Scuseria, G. E. Efficient hybrid density functional calculations in solids: Assessment of the Heyd−Scuseria−Ernzerhof screened Coulomb hybrid functional. *J. Chem. Phys.* **2004**, *121*, 1187−1192.

(40) Heil, C.; Bachelet, G. B.; Boeri, L. Absence of superconductivity in iron polyhydrides at high pressures. *Phys. Rev. B: Condens. Matter Mater. Phys.* **2018**, *97*, 214510.

(41) Fei, Y.; Ricolleau, A.; Frank, M.; Mibe, K.; Shen, G.; Prakapenka, V. Toward an internally consistent pressure scale. *Proc. Natl. Acad. Sci. U. S. A.* **2007**, *104*, 9182−9186.

(42) Dalladay-Simpson, P.; Howie, R. T.; Gregoryanz, E. Evidence for a new phase of dense hydrogen above 325 gigapascals. *Nature* **2016**, *529*, 63−67.

(43) Liermann, H.-P.; Konôpková, Z.; Morgenroth, W.; Glazyrin, K.; Bednarčik, J.; McBride, E.; Petitgirard, S.; Delitz, J.; Wendt, M.; Bican, Y. The extreme conditions beamline P02. 2 and the extreme conditions science infrastructure at PETRA III. *J. Synchrotron Radiat.* **2015**, *22*, 908−924.

(44) Prescher, C.; Prakapenka, V. B. DIOPTAS: a program for reduction of two-dimensional X-ray diffraction data and data exploration. *High Pressure Res.* **2015**, *35*, 223−230.

(45) Oishi-Tomiyasu, R. Robust powder auto-indexing using many peaks. *J. Appl. Crystallogr.* **2014**, *47*, 593−598.

(46) Le Bail, A.; Duroy, H.; Fourquet, J. Ab-initio structure determination of LiSbWO$_6$ by X-ray powder diffraction. *Mater. Res. Bull.* **1988**, *23*, 447−452.

(47) Petříček, V.; Dušek, M.; Palatinus, L. Crystallographic computing system JANA2006: general features. *Z. Kristallogr. - Cryst. Mater.* **2014**, *229*, 345−352.

(48) Gonzalez-Platas, J.; Alvaro, M.; Nestola, F.; Angel, R. EosFit7-GUI: a new graphical user interface for equation of state calculations, analyses and teaching. *J. Appl. Crystallogr.* **2016**, *49*, 1377.

(49) Kresse, G.; Hafner, J. Ab initio molecular dynamics for liquid metals. *Phys. Rev. B: Condens. Matter Mater. Phys.* **1993**, *47*, 558.

(50) Kresse, G.; Hafner, J. Ab initio molecular-dynamics simulation of the liquid-metal−amorphous-semiconductor transition in germanium. *Phys. Rev. B: Condens. Matter Mater. Phys.* **1994**, *49*, 14251.

(51) Kresse, G.; Furthmüller, J. Efficiency of ab-initio total energy calculations for metals and semiconductors using a plane-wave basis set. *Comput. Mater. Sci.* **1996**, *6*, 15−50.

(52) Blöchl, P. E.; Jepsen, O.; Andersen, O. K. Improved tetrahedron method for Brillouin-zone integrations. *Phys. Rev. B: Condens. Matter Mater. Phys.* **1994**, *49*, 16223.